Journal of Southeast University (English Edition) Vol. 31, No. 3, pp. 401 - 406 Sept. 2015 ISSN 1003—7985

Finite element modeling of pavement responses based on stress-dependent properties of asphalt layer

Dong Niya[1] Li Chang[1] Ni Fujian[1,2]

([1]School of Transportation, Southeast University, Nanjing 210096, China)

([2]Road Maintenance Technology Engineering Center of Jiangsu Province, Southeast University, Nanjing 210096, China)

Abstract: In order to investigate the stress-dependent properties of hot-mix asphalt (HMA), a dynamic modulus test was conducted on a group of AC-20 specimens at various stress states and loading frequencies, respectively. A user-defined material (UMAT) subroutine incorporating stress-dependent constitutive model was developed and finite element (FE) simulation was utilized to confirm the validity of the UMAT. A three-dimensional (3D) FE model for typical pavement structure was established, considering the HMA layer as a stress-dependent material and other layers as linear elastic materials. Periodic load was applied to the pavement model and the pavement responses were calculated, including dynamic modulus distributions, surface deflection, shear stress and tensile strain in the HMA layer, etc. Both test results and FE model predictions indicate that the dynamic modulus of asphalt concrete is sensitive to stress state and loading frequency. Using the nonlinear stress-dependent model results in greater predicted pavement responses compared with the linear elastic model. It is also found that the effects of stress-dependency on pavement responses become more significant as loading frequency decreases.

Key words: dynamic modulus test; loading frequency; stress-dependent model; user-defined material (UMAT) subroutine; pavement responses

doi: 10.3969/j.issn.1003-7985.2015.03.018

The property of stress-dependency is that the resilient modulus of a material can be affected by loading levels. For conventional design and mechanical analysis of the asphalt pavement structure, structural layers are usually simulated as linear elastic materials whose elastic moduli are constant at a certain temperature and remain unchangeable under different stress states. In fact, the pavement materials are not completely linear elastic. Nonlinear behaviors may appear as a result of complex traffic loading and environmental conditions. Asphalt layers are directly exposed to the environment and saddled with traffic loading, which results in complicated stress states, thus causing stress-dependent behavior.

To characterize stress-dependent properties, many constitutive equations have been proposed recently, and some of them have been widely used in analyzing the stress-dependent behavior of pavement materials. In recent studies, Al-Qadi et al.[1] found using the stress-dependent modulus for the unbound base layer results in great predictions of pavement responses and little estimated pavement life for rutting and fatigue cracking. By performing a dynamic modulus test, researchers found that the dynamic modulus of asphalt concrete is susceptible to confining stress and loading frequency[2]. Collop et al.[3] found that the permanent vertical strains in the stress-dependent case are significantly greater than those in the non-stress-dependent case by using a stress-dependent constitutive model for asphalt. Antes et al.[4] used the results of the triaxial testing program to model the resilient modulus of asphalt mixtures as a function of the applied stresses and found the effects of stress-dependency of asphalt mixtures to be not negligible. Zhao et al.[5] developed a stress-dependent model for asphalt mixtures based on the K-θ model and investigated the influences of stress states on dynamic modulus distribution within the surface layer. Zeiada et al.[6] found that the confining pressure affects the dynamic modulus of asphalt concrete significantly, especially at low frequencies and high temperatures. Zhao et al.[7-9] further proposed a model which employs the vertical shifting factor to characterize the pressure-dependent behavior of asphalt concrete, and the results show that when the effect of confinement is considered, the dynamic modulus can be more than two times the uniaxial value at the same temperature and frequency.

So far, the stress-dependent behavior of asphalt concrete has not received extensive research. The study presented in this paper clarifies the effect of stress-dependent asphalt concrete modulus on pavement responses.

1 Dynamic Modulus Test

In this study, basalt aggregates, filler and general 70# bitumen are used to fabricate asphalt mixture, the properties of which meet the requirements of guide of aggregate tests (JTGE20—2011). The gradation of AC-20 listed in Tab. 1 is designed in compliance with the Superpave volu-

Received 2014-12-28.

Biographies: Dong Niya (1987—), female, graduate; Ni Fujian (corresponding author), male, doctor, professor, nifujian@gmail.com.

Foundation item: Jiangsu Provincial Transportation Science and Technology Project (No. 2011Y02-1-G1).

Citation: Dong Niya, Li Chang, Ni Fujian. Finite element modeling of pavement responses based on stress-dependent properties of asphalt layer [J]. Journal of Southeast University (English Edition), 2015, 31(3): 401 - 406. [doi: 10.3969/j.issn.1003-7985.2015.03.018]

metric mixture design procedure[10]. The volumetric design of the asphalt mixture results in a bitumen content of 4.4% by weight of the total mixture to meet a 4.0% target air void.

Tab. 1 Gradation of AC-20 asphalt mixture

Gradation	Sieve size/mm										
	26.5	19	16	13.2	4.75	2.36	1.18	0.6	0.3	0.15	0.075
AC-20	100	99.3	90.2	76.6	41.3	32.9	23.9	14.6	9.6	7.6	5

First, asphalt mixtures of 150 mm × 170 mm (diameter × height) were compacted using a Superpave gyratory compactor, and then each compacted sample was cored and sawn to produce cylindrical specimens with smooth and parallel ends and the prescribed dimension of 100 mm × 150 mm (diameter × height) for use in the dynamic modulus test. The dynamic modulus test was performed in a stress-controlled compressive mode by following the general guidelines specified in *Standard Method of Test for Determining Dynamic Modulus of Hot Mix Asphalt* (AASHTO TP 62—2007). The axial loading levels were adjusted for each test condition to limit the strain levels within the range of 50 to 80×10^{-6} and the total accumulated strain within $1\,500 \times 10^{-6}$.

Dynamic moduli were measured at the confining pressures of 35, 138, and 207 kPa, the loading frequencies of 0.1, 0.5, 1, 5, 10, and 25 Hz, and the temperature of 20 ℃. Three linear variable differential transformers (LVDT) were mounted onto the surface of the specimen. Three replicates were tested for each of the 18 combinations of confining pressure and loading frequency. Before the test, specimens were conditioned at least 2 h in an air bath in order to achieve the test temperature. Dynamic modulus measurements are listed in Tab. 2. Results show that dynamic modulus increases as the loading frequency or confining stress increases, and the impact of loading frequency on dynamic modulus is greater than that of confining stress.

Tab. 2 Results of dynamic modulus E^* at 20 ℃ MPa

Confining stress/kPa	Loading frequency/Hz					
	25	10	5	1	0.5	0.1
35	10 800	8 320	7 260	4 510	3 610	1 880
138	11 500	9 150	7 700	4 860	3 910	2 150
207	12 400	9 860	8 270	5 260	4 260	2 380

2 Modeling of Stress-Dependent Behavior

The most commonly used stress-dependent constitutive model is the K-θ model shown as

$$E^* = K_1 \theta^{K_2} \tag{1}$$

where E^* is the dynamic modulus; θ is the bulk stress, which is defined as the sum of maximum principal stress, intermediate principal stress and minimum principal stress; K_1, K_2 are the coefficients. The bulk stress is equivalent to the total value of axial stress and double confining stress. The solved model coefficients are listed in Tab. 3.

In this UMAT subroutine, the stress-dependent modulus was defined as Eq. (1). The flow process of the subroutine written in Fortran language is described as follows: 1) The initial stress state and incremental strain from the main routine is obtained; 2) The overburden and horizontal stresses are calculated; 3) The total principal stress and direction are calculated; 4) The bulk stress and resilient moduli are calculated; 5) The incremental Jacobian matrices are calculated; 6) The stress tensor is updated and returned to the main routine.

Since the stress-dependent modulus is varying, the nonlinear analysis is conducted by using an incremental loading and an iterative solution technique for each loading increment[1]. An incremental Jacobian matrix (also known as incremental-stiffness matrix) in the subroutine is defined as the ratio of incremental stress to incremental strain. Using the incremental strain tensor provided by the main routine, the UMAT subroutine is required to calculate the Jacobian matrix, update the total stress tensor for the current load increment, and then transmit the updated total stress tensor to the main routine. The Jacobian matrix of material constitutive model is written as

$$\boldsymbol{D} = \begin{bmatrix} \frac{E^*(1-\mu)}{(1+\mu)(1-2\mu)} & \frac{E^*\mu}{(1+\mu)(1-2\mu)} & \frac{E^*\mu}{(1+\mu)(1-2\mu)} & 0 & 0 & 0 \\ \frac{E^*\mu}{(1+\mu)(1-2\mu)} & \frac{E^*(1-\mu)}{(1+\mu)(1-2\mu)} & \frac{E^*\mu}{(1+\mu)(1-2\mu)} & 0 & 0 & 0 \\ \frac{E^*\mu}{(1+\mu)(1-2\mu)} & \frac{E^*\mu}{(1+\mu)(1-2\mu)} & \frac{E^*(1-\mu)}{(1+\mu)(1-2\mu)} & 0 & 0 & 0 \\ 0 & 0 & 0 & \frac{E^*}{2(1+\mu)} & 0 & 0 \\ 0 & 0 & 0 & 0 & \frac{E^*}{2(1+\mu)} & 0 \\ 0 & 0 & 0 & 0 & 0 & \frac{E^*}{2(1+\mu)} \end{bmatrix} \tag{2}$$

where μ is the Poisson's ratio.

Tab. 3 The values of K-θ model coefficients for AC-20

Loading frequency/Hz	K_1	K_2	R^2
25	8.15×10^8	0.187 2	0.993 0
10	1.46×10^8	0.298 2	0.991 9
5	1.58×10^8	0.282 9	0.968 7
1	7.31×10^7	0.311 3	0.988 3
0.5	2.69×10^8	0.199 2	0.994 5
0.1	1.02×10^8	0.231 9	0.973 4

3 Verification of the UMAT Subroutine

As Fig. 1 shows, a 3D FE model dimensionally similar to the cylindrical specimen was developed by using ABAQUS Version 6.10 to confirm the validity of the UMAT subroutine. The periodic half-sine loads of different durations and amplitudes were respectively applied on the top surface. The cylindrical model was partitioned into 5 488 20-node quadratic brick elements.

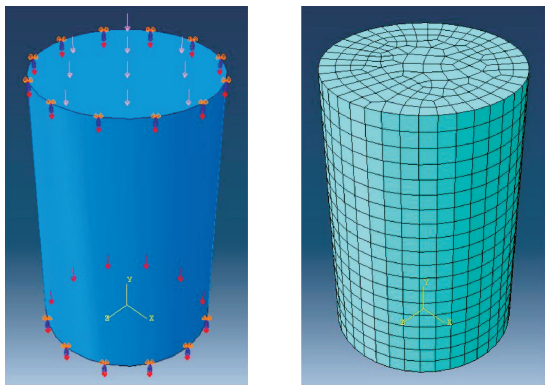

(a) (b)

Fig. 1 FE model of specimen. (a) Load application; (b) Model meshing

Tab. 4 presents the absolute error and relative error between the test measured modulus and model predicted modulus at various loading frequencies. The maximum absolute error is 132 MPa, and the corresponding relative error, which is also the maximum, is less than 7%. Results show that good agreements are achieved between test measurements and model predictions, and the nonlinear approach taken in the UMAT subroutine is confirmed to be effective.

Tab. 4 Comparisons between measured and predicted moduli

Index	Loading frequency/Hz					
	25	10	5	1	0.5	0.1
Absolute error/MPa	32	45	3	88	31	132
Relative error/%	0.28	0.49	0.04	1.81	0.79	6.14

The structural type and mechanical properties of each layer are listed in Tab. 5. The dimension of the pavement domain was 3 m × 3 m × 1.5 m (length × width × depth). The symmetrical boundary condition was considered in this pavement model and double rectangular loading areas were symmetrically distributed beside the centerline of the surface, as shown in Fig. 2(a). The traffic loading was modeled by a half-sine load of the maximum amplitude of 0.7 MPa applied on the model surface. A 20-node quadratic brick element was used for the whole model, which was partitioned into 38 640 elements. Fine meshing was used around the loading areas, while relatively coarser meshing was used as the distance and depth to the load center increased, as shown in Fig. 2(b).

Tab. 5 Structural type and mechanical properties of each layer

Structural layer	Material type	Depth/cm	Modulus/MPa	Density/(kg · m^{-3})	Poisson ratio
Surface	AC	18	Stress-dependent	2 560	0.35
Base	CTB	34	1 500	2 300	0.25
Sub-base	LFS	20	750	2 300	0.25
Subgrade	SG		40	1 800	0.40

Notes: CTB represents the cement-treated base; LFS represents the lime and fly-ash stabilized soil.

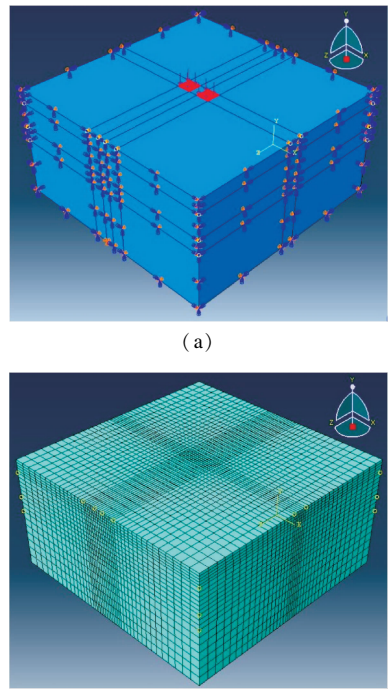

(a)

(b)

Fig. 2 Pavement FE model. (a) Load application; (b) Model meshing.

4 Result and Analysis

The horizontal distributions of dynamic modulus at various transverse sections of the HMA layer at a loading frequency of 10 Hz and the vertical distributions at various loading frequencies are plotted in Figs. 3(a) and (b), respectively. The maximum predicted modulus is observed at the surface of the HMA layer under the center of each loading area. The predicted modulus varies both horizontally and vertically due to the fact that the stress state alters throughout the HMA layer. It is evident that the predicted modulus decreases sharply as the horizontal distance to the load center increases. In most cases, the

predicted modulus within the loading area decreases as vertical depth increases, with the exception of the area around the wheel gap center. The trends of predicted modulus observed in Fig. 3(b) are reasonable and in accordance with expectations. The predicted modulus under the load center decreases as the vertical depth increases. The reduction of the predicted modulus becomes more significant when the pavement is loaded at a high frequency.

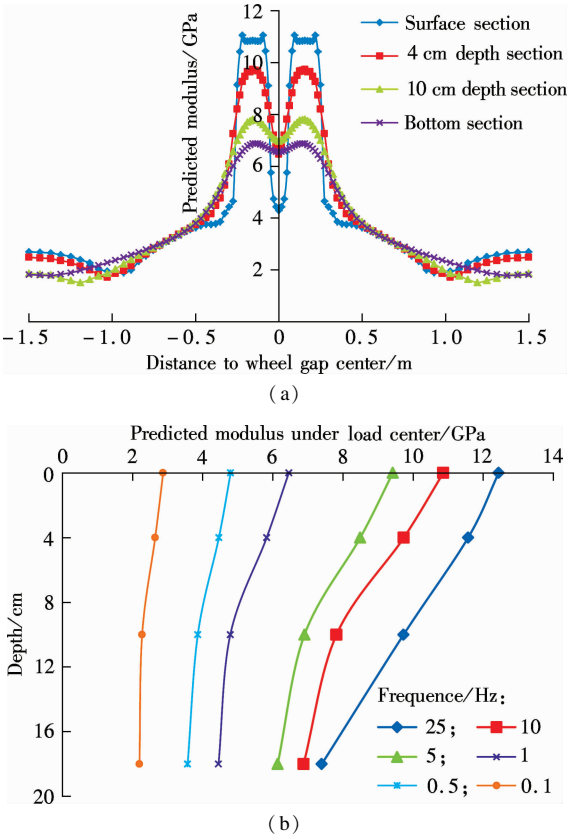

Fig. 3 Distributions of the predicted modulus. (a) Horizontal distributions at various sections at 10 Hz; (b) Vertical distributions at different loading frequencies

As shown in Fig. 4, the maximum deflection is observed under the center of each loading area, and surface deflection increases as the loading frequency decreases. However, there are no obvious differences in the deflection basin curve within a range of loading frequencies (1 to 10 Hz). In contrast, the augment of the maximum deflection is significant when the loading frequency varies from 25 to 10 Hz or 0.5 to 0.1 Hz. The results demonstrate that surface deflection is sensitive to the loading frequency, especially above 10 Hz or below 0.5 Hz.

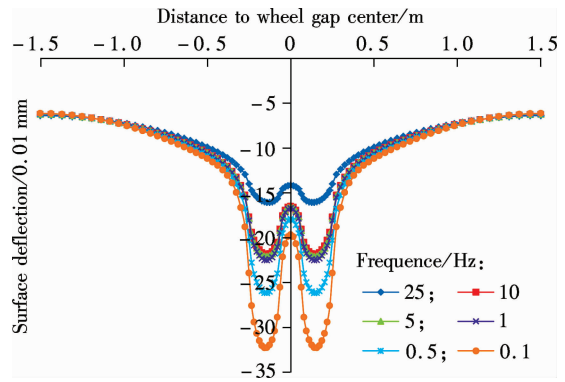

Fig. 4 Surface deflection basins at different loading frequencies

In this study, the shear stress specifically represents the maximum shear stress, which value is equivalent to the difference between the maximum principal stress and the minimum principal stress. As shown in Fig. 5(a), when the pavement is loaded at 25 Hz, the shear stress close to the surface is positive owing to the fact that the minimum principal stress is greater than the maximum principal stress; as depth increases, the shear stress gradually turns to negative and shares a similar development with other loading conditions. Apart from this exception, the shear stress increases in the upper portion of the surface layer, then decreases in the lower part. The shear stress increases as the loading frequency decreases. The maximum shear stresses at each loading frequency are all observed at 7 cm depth of the HMA layer. With the loading frequency varying from 25 to 0.1 Hz, the maximum shear stress increases by 20%.

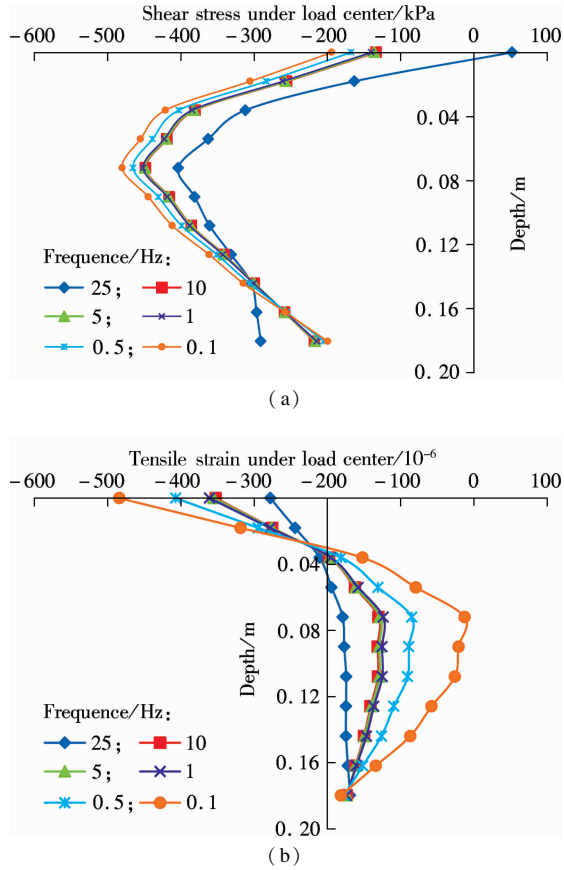

Fig. 5 Vertical distributions. (a) Shear stresses; (b) Tensile strains at various loading frequencies

Fig. 5(b) illustrates the vertical distributions of tensile strains within the HMA layer at various loading frequencies. The change in tensile strain consists of three stages. At beginning, the tensile strain gradually increases from negative to zero. Then, it constantly increases

from zero to the maximum. Finally, it decreases as the vertical depth increases. However, the third stage at 25 Hz is inconspicuous, and it remains fundamentally unchanged. It is clear that the lower the loading frequency, the greater the tensile strain (absolute value). The maximum tensile strain increases 8.3 times when the loading frequency varies from 25 to 0.1 Hz, but the differences in the tensile strain are small at loading frequencies of 1 to 10 Hz. From the above, the impact of the loading frequency on tensile strain within the HMA layer is remarkable, especially at low loading frequencies.

Tab. 6 summarizes the predicted pavement responses at selected positions based on the linear elastic and nonlinear stress-dependent models at various loading frequencies. It is apparent that all types of model predictions listed in the table become greater as the loading frequency decreases. The use of the nonlinear stress-dependent model for the HMA layer leads to greater predicted pavement responses in comparison with the linear elastic model. It is found that the maximum pavement responses are all achieved from the stress-dependent model at 0.1 Hz, indicating that the effects of stress-dependency in asphalt concrete and frequency of traffic loading are significant for pavement responses.

Tab. 6 Comparisons of predicted pavement responses between linear and nonlinear models

Loading frequency/Hz	Model type	Maximum deflection at surface/mm	Compressive strain on top of subgrade/10^{-6}	Tensile strain in bottom of HMA/10^{-6}	Maximum shear stress in HMA/kPa	Tensile stress at bottom of base/kPa	Tensile stress at bottom of subbase/kPa
0.1	L	0.183	460.9	47.2	472.3	58	40.8
	NL	0.323	502.9	269.9	511.9	69.2	56.9
0.5	L	0.154	443.8	38.2	446.6	52	34
	NL	0.262	489.8	164.1	501.3	66	51.9
1	L	0.146	438.4	36.4	435.7	49.8	31.7
	NL	0.225	478.6	106	491.3	63.1	47.7
5	L	0.133	427.8	32.7	427.7	44.8	27.1
	NL	0.221	477.1	99.7	489.8	62.6	47.1
10	L	0.129	424.1	31.3	415.1	42.8	25.5
	NL	0.219	476.3	92.6	487.0	62.4	46.8
25	L	0.124	419.4	29.6	361.9	40.1	23.3
	NL	0.161	448.0	62.9	414.6	53.6	35.7

Notes: L represents linear elastic model; NL represents nonlinear stress-dependent model.

5 Conclusion

Based on the predicted pavement responses obtained from different constitutive models, conclusions can be drawn as follows:

1) Using the nonlinear stress-dependent model results in greater predicted pavement responses than using the linear elastic model, including surface deflection, shear stress and tensile strain in the HMA layer, tensile stresses at the bottom of the base and sub-base, and compressive strain at the top of the subgrade.

2) Predicted pavement responses increase as the loading frequency decreases. However, it is found that sensitivity to loading frequencies of 1 to 10 Hz is less compared to other loading frequencies.

3) The effects of stress-dependency on surface deflection and tensile strain in the HMA layer become more significant as the loading frequency decreases.

References

[1] Al-Qadi I, Wang H, Tutumluer E. Dynamic analysis of thin asphalt pavements by using cross-anisotropic stress-dependent properties for granular layer [J]. *Transportation Research Record*, 2010, **2154**: 156 - 163.

[2] Ma X, Ni F J, Chen R S. Dynamic modulus test of asphalt mixture and prediction model [J]. *China Journal of Highway and Transport*, 2008, **21**(3): 35 - 39. (in Chinese)

[3] Collop A C, Scarpas A, Kasbergen C, et al. Development and finite element implementation of stress-dependent elastoviscoplastic constitutive model with damage for asphalt [J]. *Transportation Research Record*, 2003, **1832**: 96 - 104.

[4] Antes P W, Van Dommelen A E, Houben J M, et al. Stress-dependent behavior of asphalt mixtures at high temperatures [C]//*Proceedings of the Technical Sessions*. Lexington, USA: Association of Asphalt Paving Technologist, 2003, **72**: 173 - 195.

[5] Zhao Y Q, Tan Y Q, Yu X. Stress-dependent mechanical behavior of asphalt mixtures [J]. *Journal of Huazhong University of Science and Technology: Natural Science Edition*, 2010, **38**(10): 124 - 127. (in Chinese)

[6] Zeiada W, Kaloush K, Biligiri K, et al. Significance of confined dynamic modulus laboratory testing for asphalt concrete: conventional, gap-graded, and open-graded mixtures [J]. *Transportation Research Record*, 2011, **2210**: 9 - 19.

[7] Zhao Y Q, Tang J, Liu L. Construction of triaxial dynamic modulus master curve for asphalt mixtures [J]. *Construction and Building Materials*, 2012, **37**(12): 21 - 26.

[8] Zhao Y Q, Liu H, Liu W. Characterization of linear viscoelastic properties of asphalt concrete subjected to confining pressure [J]. *Mechanics of Time-Dependent Materi-*

als, 2013, **17**(3): 449 - 463.
[9] Zhao Y Q, Bai L, Liu H. Implementation of a triaxial dynamic modulus master curve in finite-element modeling of asphalt pavements [J]. *Journal of Materials in Civil Engineering*, 2014, **26**(3): 491 - 498.
[10] AASHTO R 35-04. Standard practice for Superpave volumetric design for hot mix asphalt (HMA) [R]. Washington DC: American Association of State Highway and Transportation Officials, 2004.

基于沥青面层应力依赖性的路面响应有限元模拟

董尼娅[1] 李 昶[1] 倪富健[1,2]

([1] 东南大学交通学院,南京 210096)
([2] 东南大学江苏省道路养护工程技术研究中心,南京 210096)

摘要: 为了探究沥青混合料的应力依赖性质,分别在不同应力状态及荷载频率下对一组 AC-20 试件进行了动态模量试验. 开发了一个包含应力依赖本构模型的用户自定义材料子程序并利用有限元模拟证实了其有效性. 建立了一个典型路面结构的三维有限元模型,将沥青面层视为应力依赖性材料,而其他结构层为线弹性材料. 对路面模型施加周期性荷载,并计算得到路面响应,包括动态模量的分布、路表弯沉、沥青面层的剪应力及拉应变等. 试验结果及有限元模型预测值均表明了沥青混凝土的动态模量对应力状态及荷载频率具有敏感性. 与线弹性模型相比,使用非线性应力依赖模型得到的预测路面响应更大;应力依赖性对路面响应的影响随着荷载频率的减小变得更加显著.

关键词: 动态模量试验;荷载频率;应力依赖性模型;UMAT 子程序;路面响应
中图分类号: U416. 217